LAWRENCE
LIVERMORE
NATIONAL
LABORATORY

UCRL-JRNL-229471

MULTIPLE SYNTHESIS ROUTES TO TRANSPARENT CERAMIC LUTETIUM ALUMINUM GARNET

J. D. Kuntz, J. J. Roberts, M. E. Hough, N. J. Cherepy

March 28, 2007

Scripta Materialia

MARCH 20, 2007

MULTIPLE SYNTHESIS ROUTES TO TRANSPARENT CERAMIC LUTETIUM ALUMINUM GARNET

Joshua D. Kuntz[1], Jeffery J. Roberts[2],
Meghan Hough[1], & Nerine J. Cherepy[1]

[1]Chemistry, Materials and Life Sciences
[2]Energy & Environment
Lawrence Livermore National Laboratory

ABSTRACT

Transparent ceramics may be fabricated via using various material sources and processing routes. In an effort to identify key processing parameters, we explored two different particle processing methods for production of ceramic lutetium aluminum garnet doped with cerium (LuAG:Ce): flame spray pyrolysis powder and high-energy-milled commercial powders. Powders were cold-pressed and vacuum sintered prior to hot isostatic pressing. The flame spray pyrolysis route led to phase-pure transparent ceramics, while the high-energy milling route led to multi-phase, translucent ceramics.

KEYWORDS

optical materials, ceramics, sintering, mechanical milling, hot isostatic pressing (HIP)

INTRODUCTION

Requirements for scintillator crystals include a high effective atomic number (Z), high, proportional light yield, fast decay, and high transparency. Lutetium aluminum garnet doped with cerium (LuAG:Ce) satisfies these requirements, although the intrinsic radioactivity of Lu compromises its utility for certain applications. LuAG is an excellent model system for demonstration of scintillator functionality, since ceramic LuAG can be directly compared to single crystal LuAG[1], this is in contrast to some candidate scintillator ceramics that are not easily growable as single crystals. Transparent polycrystalline ceramics have advantages over single crystal materials due to the possibility to increase activator concentration and uniformity over that achievable in a melt-grown crystal. Additionally, ceramics exhibit improved mechanical properties compared to single crystals, leading to more robust detector devices. Recently, Li et al. (2005)[2] produced transparent ceramic LuAG:Ce through a solid state reaction of Lu_2O_3, Al_2O_3, and CeO_2 nanopowders, both Liao et al. (2005)[3] and Li et al. (2006)[4] fabricated transparent ceramic LuAG:Ce from co-precipitated mixed metal-oxide powders, and Liu et al. (2006)[5] used a nitrate-glycine combustion method. In our earlier work, Cherepy et al. (2007)[1] demonstrated transparent ceramic LuAG:Ce using a nanoparticles synthesized by a citrate combustion method. .

In the present work, two synthesis routes were utilized to produce LuAG:Ce polycrystalline ceramics. The first employed stoichiometric mixed metal oxide particles synthesized via flame spray pyrolysis. The second was a reactive sintering approach, in which commercial powders of simple oxides were subjected to high-energy milling, followed by solid-state reaction during sintering. The two processing methods were used to create powders with the composition $Lu_{2.98}Ce_{0.02}Al_5O_{12}$ (LuAG:Ce). This provides for a dopant level of 0.67 mol% Ce in

the Lu site. Ultimately, the most economically feasible fabrication route for transparent ceramics will require high yields of transparent optics, scaleable methods, and minimization of processing steps. Our intention in this study is the exploration of two very different methodologies in order to identify promising directions for transparent ceramics development.

EXPERIMENTAL PROCEDURE

Flame spray pyrolysis (FSP)

Flame spray pyrolysis, as described by Madler et al. (2002)[6] and Pratsinis (1996, 1998)[7, 8], was used to synthesize LuAG:Ce powder. Nanoparticles synthesized using the flame spray pyrolysis method are found to have a narrow particle size distribution, uniform composition, and highly spherical particles exhibiting little to no agglomeration. Precursors were prepared by dissolving stoichiometric amounts of metal salts in organic solvents. The lutetium, aluminum, and cerium salts, in the form of hydrated acetylacetonate, were dissolved in a solvent cocktail of ethyl hexanoic acid, acetonitrile, and acetic anhydride in a 1:1:1 ratio by volume. The resulting solution was atomized with oxygen and injected into a methane/oxygen flame. The organic solvents and metal salts combust in the flame, creating nano-scale particles that are collected using a filter plate. Due to the lean conditions in the flame and oxygen atomization gas used in the processing technique, no further purification steps are necessary.

High-energy ball-milling (HEBM)

LuAG:Ce powders were prepared for reactive sintering from commercial sources. Lutetium, in the form of 99.99% pure micron-scale Lu_2O_3 powder (Alfa Aesar), and aluminum, in the form of Al_2O_3 nanopowder with an average particle size of 20 nm and a purity of 99.97% (Nanostructured and Amorphous Materials, Inc.), were combined in the appropriate

stoichiometry along with deionized water to form a mixture. Cerium nitrate hexahydrate, 99.999% pure (Sigma-Aldrich) was added to reach the desired dopant concentration. The resultant slurry was milled in a Szegvari attritor (model 01-HD, Union Process, Inc.) with zirconia milling media at a weight ratio of 55:1 (ball to powder) for 4 hours at 15°C. To prevent composition inhomogeneities, due to settling of the denser lutetia particles, the resulting suspension was dried while stirring. The dried powder mixture was then ground and calcined at 800°C to decompose the cerium nitrate to ceria and remove any organic contaminants.

Sintering & Post-processing

Powders from the two synthesis methods were used to prepare green bodies. The samples were uniaxially cold-pressed to 125 MPa, loaded into a vacuum furnace, and evacuated until the vacuum was below 2×10^{-6} torr. The furnace was heated rapidly to 1100°C, then held for 30 minutes to restore vacuum to the previous level before rising to a hold temperature of 1800°C. The dwell time at temperature was 8 hours. The flame spray pyrolysis and reactively sintered samples were then subjected to hot isostatic pressing (HIP). HIP is a process in which a gas applies isostatic pressure to a part at temperatures high enough to allow for creep-deformation of the material, in this case, to remove residual porosity. The HIP conditions were argon gas as the pressure medium at 207 MPa, a hold temperature of 1800°C, and duration of three hours. Since the samples were previously vacuum sintered to closed porosity, no canning of the samples was required prior to HIP.

Optical and Radioluminescence Characterization

Optical absorption spectra were acquired using a Perkin-Elmer Lambda 19 spectrophotometer. Radioluminescence spectra were acquired using a ^{90}Sr beta source and a

Princeton Instruments/Acton Spec 10 spectrograph coupled to a thermoelectrically cooled CCD camera.

RESULTS & DISCUSSION

In an effort to understand how the properties of the powder precursor affect the final ceramics, we undertook ceramic fabrication with two very different feedstock materials. All attempts were made to reproduce processing conditions, so that the only variable was the particle feedstock, in order to study how the physical properties of the feedstock affect the ceramic product. The Flame Spray Pyrolysis (FSP) particles are stoichiometric and have a narrow particle size distribution. The High Energy Ball-Milled (HEBM) simple oxides start with larger primary particles, and undergo reactive sintering during heat treatment to form the stoichiometric ceramics.

Flame Spray Pyrolysis Powder

The FSP method resulted in a free flowing low tap-density powder, with a narrow particle size range of smooth spheres, and only a light degree of agglomeration, Figure 1. These characteristics are highly desired for the production of uniform green bodies. In fact, the uniaxially pressed green bodies from FSP material are already translucent before sintering. This indicates very uniformly packed particles with very fine pore structure. The XRD data, Figure 2, reveals extremely broad peaks, indicating very fine crystallites with amorphous qualities. The few peak locations present do not directly match any of the available powder diffraction files corresponding to the possible phase combinations of the constituent elements.

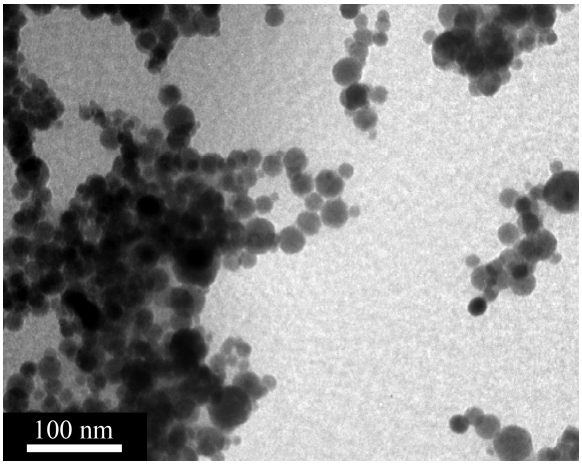

Figure 1. TEM micrograph of FSP particles, as produced, with an average particle size of 30 nm.

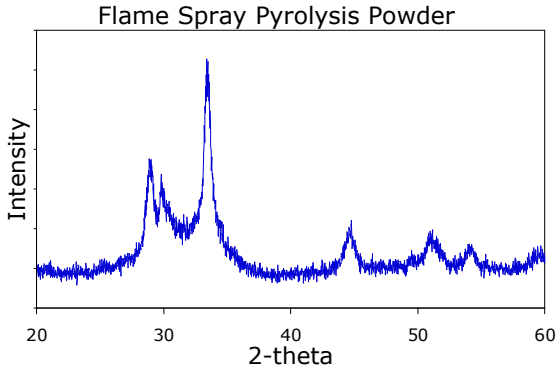

Figure 2. XRD pattern of FSP particles as produced.

High-energy Ball-milled Powder

The powders used for the reactively sintered samples started out with grossly disparate particle sizes. The alumina was in the form of fine nanoparticles with an average particle size of 20 nm, while the lutetia consisted of coarser micron-sized particles. This size variation combined with the significant disparity in the materials' densities resulting in difficulties in creating a homogeneous mixture. This required the use of an attrition mill to simultaneously refine the particle size of the lutetia, break up agglomerates of alumina, and combine the two phases in a uniform mixture. The material morphology after a calcination step at 800ºC can be seen in Figure 3. It is apparent from the TEM image that the lutetia, the darker particles, has been

reduced in size to the submicron range while simultaneously uniformly distributed with the alumina, the lighter particles. It is interesting to note the XRD pattern for the calcined powder, Figure 4, displayed lines only from Lu_2O_3. This is likely due to the significant x-ray interactions with the higher Z material.

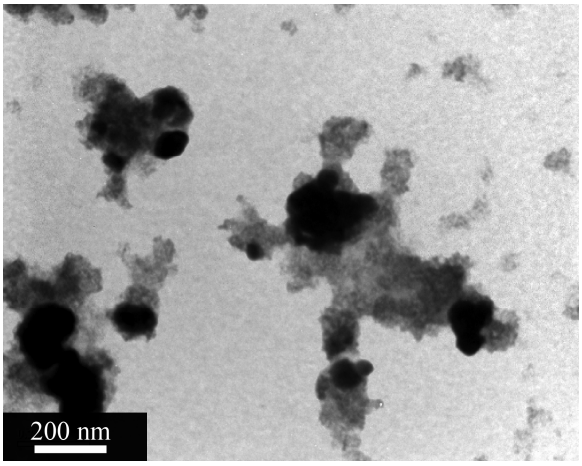

Figure 3. TEM micrograph of high-energy ball-milled particles after calcination at 800ºC. The alumina has an average particle size of 20 nm and the darker lutetia particles average 150 nm.

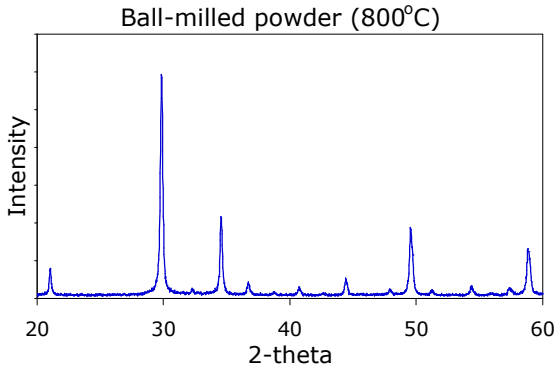

Figure 4. XRD pattern of high-energy ball-milled particles after calcination at 800ºC.

Consolidated Ceramic Samples

After vacuum sintering at 1800ºC for eight hours, the samples were ground and polished for subsequent evaluation. The images of the samples, backlit over text in Figure 5, reveal significant differences between the samples. Those made from FSP powders result in highly transparent ceramics, although with significant residual porosity (98.7% dense), while the samples made from high-energy ball-milled powders resulted in translucent samples with much finer residual porosity (>99% dense). Another significant variation between the samples is

revealed through X-ray diffraction. Figure 6 reveals that both feedstock sources result in the formation of LuAG, although the HEBM/reactively sintered sample also exhibits a minor phase of lutetia (peaks indicated by asterisks). The multiple phase nature of the HEBM/reactively sintered samples is verified through microstructural evaluation. It is unlikely that the starting composition of the HEBM powder led to the second phase because the powders were measured to within 100 ppm. It is more probable that alumina was preferentially lost during the subsequent processing steps, since the finer particles are more likely to adhere to the milling media and grinding container. It may be possible to fabricate phase-pure LuAG ceramics following the same processing conditions, correcting for the observed sub-stoichiometric conditions in the final ceramics by addition of a slight excess of alumina during milling.

After polishing, samples from both material production routes were thermally etched at 1650ºC for 60 minutes. This allowed for evaluation of microstructural features using SEM. The FSP sample has equiaxed grains ranging in size from 1 to 15 microns with residual intergranular porosity, Figure 7. Similarly, the HEBM/reactively sintered sample has equiaxed LuAG grains in the same size range along with an intergranular porosity, Figure 8. The HEBM/reactively sintered samples also have an intergranular second phase, Figure 9, which can be assumed to be Lu_2O_3 from the XRD patterns from Figure 6.

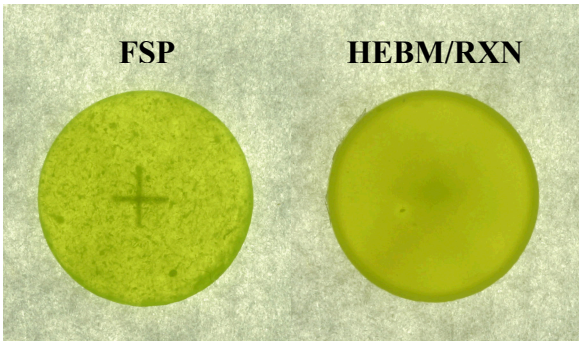

Figure 5. Images of LuAG:Ce samples after vacuum sintering.

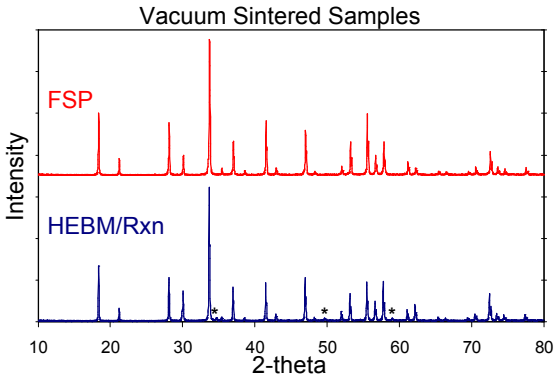

Figure 6. XRD of vacuum sintered samples.

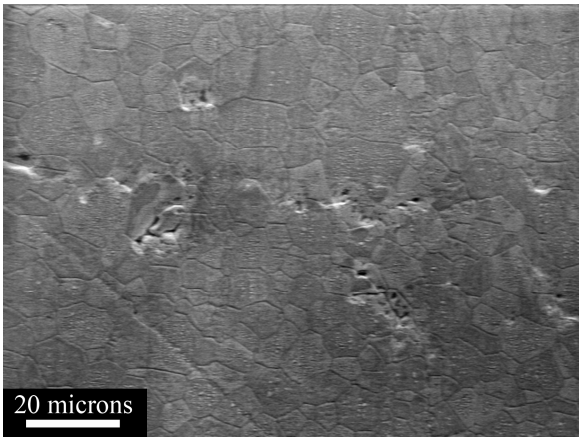

Figure 7. SEM micrograph of thermally etched FSP sample after vacuum sintering with an average grain size of ~10 microns.

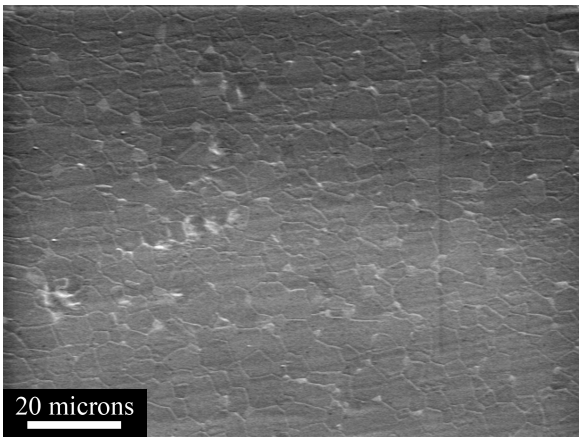

Figure 8. SEM micrograph of thermally etched HEBM/RXN sample after vacuum sintering with an average grain size of ~5 microns.

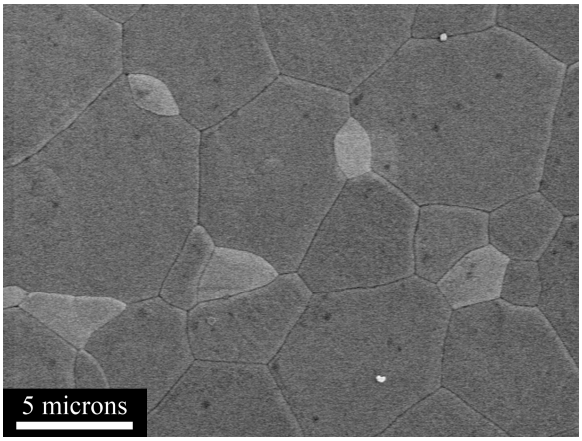

Figure 9. SEM micrograph of thermally etched HEBM/RXN sample from Figure 8 after vacuum sintering, showing the second phase assumed to be Lu_2O_3 (lighter grains).

The disparity in optical quality of the samples became more pronounced after the HIP'ing step. For this process the samples were heated to 1800ºC, well beyond the temperature needed to allow for creep of the ceramic matrix, and inert gas pressure was applied to eliminate the closed porosity. Optical images, Figure 10, show the significant improvement of optical clarity in the FSP sample after HIP'ing, while the HEBM/reactively sintered sample did not show significant improvement. Subsequent evaluation by XRD and SEM revealed no significant changes to the

samples besides reduced porosity. The XRD patterns were unchanged and micrographs indicated only a small degree of grain growth.

While the FSP ceramic is highly transparent, approaching single crystal clarity, the HEBM ceramic exhibits significant scatter. Figure 11 shows the optical absorption spectrum of the FSP ceramic, along with luminescence spectra of the two ceramics. The absorption spectrum of LuAG:Ce shows the characteristic Ce^{3+} absorption bands at 340 and 450 nm. The beta-excited radioluminescence has the characteristic peaks at 512 and 547 nm due to the splitting of the Ce^{3+} 4f ground state. Interestingly, the relative intensities of these two bands differs between the FSP and HEBM ceramics, with the FSP ceramic exhibiting a spectrum very similar to the single crystal and the HEBM ceramic luminescence showing stronger relative luminescence in the 547 nm band.

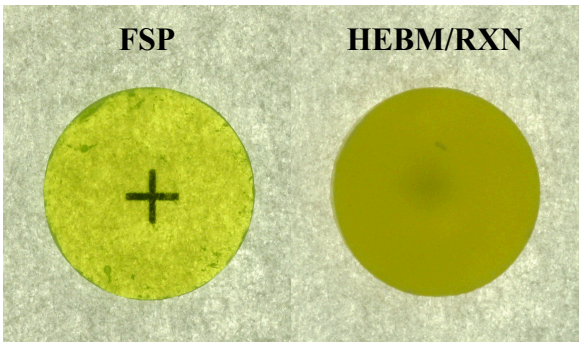

Figure 10. Images of LuAG:Ce samples after HIP.

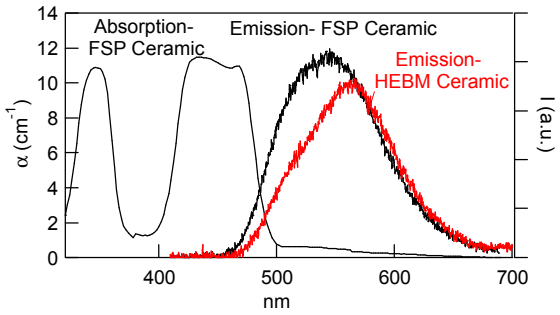

Figure 11. Optical absorption of the FSP ceramic shows transparency similar to that of single crystal LuAG, with strong absorption bands corresponding to Ce3+. Beta-excited radioluminescence of the two ceramics reveals the characteristic Ce3+ luminescence.

CONCLUSIONS

Vacuum sintering followed by hot isostatic pressing provides a processing route to dense ceramics parts with low levels of porosity. However, particle feedstock and processing conditions must be optimized to achieve high optical transparency in ceramics. Flame spray pyrolysis produces spherical powder particles with inherently uniform composition, even in complex mixed metal oxide systems. This allows for excellent control over the final phase purity and thus the final transparency of the samples. On the other hand, high-energy ball-milling can generate compositional variations due to materials losses. In phases with narrow compositional ranges, like garnets, this can cause a secondary phase to form in the specimens. Since the only detectable variation between the FSP and HEBM/reactively sintered specimens was the presence of a second phase in the latter, we can conclude that the excess lutetia creates the decreased transparency in the finished samples due to scattering at phase boundaries. Additional studies of the radioluminescence and applications to radiation detection will be published elsewhere [9].

ACKNOWLEDGMENTS

This work was supported by the Domestic Nuclear Detection Office of the Department of Homeland Security. The authors would like to thank Prof. Sotiris Pratsinis and

Dr. Reto Strobel from the Particle Technology Laboratory at ETH Zurich for their shared expertise in flame spray pyrolysis and also Dr. Natalia Zaitseva for transmission electron microscopy and William Ralph for photography. This work was performed under the auspices of the U.S. Department of Energy by University of California, Lawrence Livermore National Laboratory under Contract W-7405-Eng-48.

REFERENCES

[1] N. J. Cherepy, J. D. Kuntz, T. M. Tillotson, D. T. Speaks, S. A. Payne, B. H. T. Chai, Y. Porter-Chapman, S. E. Derenzo, , Nuclear Instruments and Methods: A (2007) In Press.H. L. Li,
[2] X. J. Liu, L. P. Huang, Journal of the American Ceramic Society 88 (2005) 3226.
[3] Y. K. Liao, D. Y. Jiang, J. L. Shi, Materials Letters 59 (2005) 3724.
[4] H. L. Li, X. J. Liu, R. J. Xie, Y. Zeng, L. P. Huang, Journal of the American Ceramic Society 89 (2006) 2356.
[5] X. J. Liu, H. L. Li, R. J. Xie, N. Hirosaki, X. Xu, L. P. Huang, Journal of Materials Research 21 (2006) 1519.
[6] L. Madler, H. K. Kammler, R. Mueller, S. E. Pratsinis, Journal of Aerosol Science 33 (2002) 369.
[7] S. E. Pratsinis, Progress in Energy and Combustion Science 24 (1998) 197.
[8] S. E. Pratsinis, S. Vemury, Powder Technology 88 (1996) 267.
[9] G. Hull, T. Niedermayr, A. Drobshoff, S. Payne, and N. Cherepy, Nuclear Instruments and Methods: A (2007) In Press.